Table 4 Changes in angiogenesis-related factors in plasma

Factor	*n*		At baseline	At the end of cycle 1	Reduction rate (%)	*p* value*
Plasma VEGF (pg/mL)	17	Mean ± SD	48.7 ± 62.6	37.5 ± 10.2	−7.0 ± 40.1	0.531
		Median	31.0	31.0	0.0	
		Range	31–291	31–65	−109.7 to 87.3	
t-PA (ng/mL)	17	Mean ± SD	7.4 ± 3.4	7.8 ± 5.2	−3.3 ± 27.0	0.991
		Median	7.5	6.5	4.8	
		Range	3–16	3–25	−55.8 to 35.6	
VCAM-1 (ng/mL)	17	Mean ± SD	432.9 ± 172.6	444.4 ± 164.7	−4.3 ± 19.4	0.782
		Median	369.0	413.0	−3.8	
		Range	249.0–982.0	269.0–841.0	−44.9 to 21.2	
PAI-1 (ng/mL)	17	Mean ± SD	21.5 ± 16.4	21.7 ± 12.2	−8.3 ± 32.6	0.530
		Median	18.0	17.0	0.0	
		Range	10.0–81.0	10.0–54.0	−80.0 to 50.6	

* Wilcoxon signed rank sum test

Table 5 Major adverse drug reactions (highest grade per event per patients). The ADRs listed here were reported in >35% of patients

ADR	Grade								Total ($n = 19$)	
	1	%	2	%	3	%	4	%	*n*	%
Hematologic										
Neutropenia			1	5.3	6	31.6	11	57.9	18	94.7
Leukopenia			1	5.3	12	63.2	5	26.3	18	94.7
Hemoglobin decreased	5	26.3	5	26.3	2	10.5			12	63.2
Thrombocytopenia	6	31.6	1	5.3					7	36.8
Non-hematologic										
Nail disorder	10	52.6	4	21.1					14	73.7
Malaise	8	42.1	6	31.6					14	73.7
Dysgeusia	11	57.9	2	10.5					13	68.4
Alopecia	1	5.3	12	63.2					13	68.4
Edema	4	21.1	7	36.8	1	5.3			12	63.2
Anorexia	5	26.3	6	31.6					11	57.9
Diarrhoea	6	31.6	4	21.1					10	52.6
Nausea	7	36.8	4	21.1					11	57.9
Vomiting	6	31.6	1	5.3	1	5.3			8	42.1
Stomatitis	4	21.1	3	15.8					7	36.8

Acknowledgments We are grateful to Yutaka Ariyoshi, Yuh Satata, Tomohide Tamura, Kojiro Shimozuma, Seigo Nakamura, and Yuichi Watanabe for extramural review. We thank Junichi Yonezawa Toyomitsu Sato, Masahito Komuro, Kentaro Nagai, Hiroshi Nakayama, Yuji Takami, Itsumi Takaya, Akira Fukushima, Katsuo Ohwada, Kenzo Iizuka, and Kiyoshi Eshima for assistance in data collection and analysis.

References

1. Carmeliet P, Jain RK. Principles and mechanisms of vessel normalization for cancer and other angiogenic diseases. Nat Rev Drug Discov. 2011;10:417–27.
2. Weidner N, Folkman J, Pozza F, Bevilacqua P, Allred EN, Moore DH, et al. Tumor angiogenesis: a new significant and independent prognostic indicator in early-stage breast carcinoma. J Natl Cancer Inst. 1992;84:1875–87.
3. Ferrara N. Pathways mediating VEGF-independent tumor angiogenesis. Cytokine Growth Factor Rev. 2010;21:21–6
4. Marty M, Pivot X. The potential of anti-vascular endothelial growth factor therapy in metastatic breast cancer: clinical experience with anti-angiogenic agents, focusing on bevacizumab. Eur J Cancer. 2008;44:912–20.
5. Miller K, Wang M, Gralow J, Dickler M, Cobleigh M, Perez EA, Davidson NE, et al. Paclitaxel plus bevacizumab versus paclitaxel alone for metastatic breast cancer. N Engl J Med. 2007;357:2666–76.

6. Miles D, Chan A, Romieu G, Dirix LY, Cortes J, Pivot X, et al. Phase III study of bevacizumab plus docetaxel compared with placebo plus docetaxel for the first-line treatment of human epidermal growth factor receptor 2-negative metastatic breast cancer. J Clin Oncol. 2010;28:3239–47.
7. Hurwitz H, Fehrenbacher L, Novotny W, Cartwright T, Hainsworth J, Heim W, et al. Bevacizumab plus irinotecan, fluorouracil, and leucovorin for metastatic colorectal cancer. N Engl J Med. 2004;350:2335–42.
8. Sandler A, Gray R, Perry MC, Brahmer J, Schiller JH, Dowlati A, et al. Paclitaxel–carboplatin alone or with bevacizumab for non-small-cell lung cancer. N Engl J Med. 2006;355:2542–50.
9. Benjamin LE, Golijanin D, Itin A, Pode D, Keshet E. Selective ablation of immature blood vessels in established human tumors follows vascular endothelial growth factor withdrawal. J Clin Invest. 1999;103:159–65.
10. Abramsson A, Lindblom P, Betsholtz C. Endothelial and non-endothelial sources of PDGF-B regulate pericyte recruitment and influence vascular pattern formation in tumors. J Clin Invest. 2003;112:1142–51
11. Ostman A, Heldin CH. PDGF receptors as targets in tumor treatment. Adv Cancer Res. 2007;97:247–74.
12. Morikawa S, Baluk P, Kaidoh T, Haskell A, Jain RK, McDonald DM. Abnormalities in pericytes on blood vessels and endothelial sprouts in tumors. Am J Pathol. 2002;160:985–1000.
13. Laird AD, Vajkoczy P, Shawver LK, Thurnher A, Liang C, Mohammadi M, et al. SU6668 is a potent antiangiogenic and antitumor agent that induces regression of established tumors. Cancer Res. 2000;60:4152–60.
14. Machida S, Saga Y, Takei Y, Mizuno I, Takayama T, Kohno T, et al. Inhibition of peritoneal dissemination of ovarian cancer by tyrosine kinase receptor inhibitor SU6668 (TSU-68). Int J Cancer. 2005;114(2):224–9.
15. Naumova E, Ubezio P, Garofalo A, Borsotti P, Cassis L, Riccardi E, et al. The vascular targeting property of paclitaxel is enhanced by SU6668, a receptor tyrosine kinase inhibitor, causing apoptosis of endothelial cells and inhibition of angiogenesis. Clin Cancer Res. 2006;12:1839–49.
16. Yonekura K, Basaki Y, Fujita H, Chikahisa L, Hashimoto A, Cherrington J, et al. Inhibition of VEGF/KDR signaling by TSU-68 (SU6668), an oral anti-angiogenic agent, can synergistically enhance the anti-tumor activity of taxol: a new paradigm for breast cancer chemotherapy. Breast Cancer Res Treat. 2001;69(3):216(abstr29).
17. Murakami H, Ueda Y, Shimoyama T, Yamamoto N, Yamada Y, Arioka H, et al. Phase I, pharmacokinetic, and biological studies of TSU-68, a novel multiple receptor tyrosine kinase inhibitor, administered after meals with solid tumors. Cancer Chemother Pharmacol. 2011;67:1119–28.
18. Therasse P, Arbuck SG, Eisenhauer EA, Wanders J, Kaplan RS, Rubinstein L, et al. New guidelines to evaluate the response to treatment in solid tumors. European Organization for Research and Treatment of Cancer, National Cancer Institute of the United States, National Cancer Institute of Canada. J Natl Cancer Inst. 2000;92:205–16.
19. Common Toxicity Criteria v 2.0: cancer therapy evaluation program, National Cancer Institute, Bethesda, MD. 1999.
20. Ando M, Watanabe T, Nagata K, Narabayashi M, Adachi I, Katsumata N. Efficacy of docetaxel 60 mg/m^2 in patients with metastatic breast cancer according to the status of anthracycline resistance. J Clin Oncol. 2001;19:336–42.
21. Taguchi T, Furue H, Niitani H, Ishitani K, Kanamaru R, Hasegawa K, et al. Phase I clinical trial of RP56976 (docetaxel) a new anticancer drug. Jpn J Cancer Chemother. 1994;21:1997–2005 (in Japanese, abstract in English).
22. Motzer RJ, Hutson TE, Tomczak P, Michaelson MD, Bukowski RM, Rixe O, et al. Sunitinib versus interferon alfa in metastatic renal-cell carcinoma. N Engl J Med. 2007;356:115–24.
23. Llovet JM, Ricci S, Mazzaferro V, Hilgard P, Gane E, Blanc JF, et al. Sorafenib in advanced hepatocellular carcinoma. N Engl J Med. 2008;359:378–90.
24. Feldman DR, Baum MS, Ginsberg MS, Hassoun H, Flombaum CD, Velasco S, et al. Phase I trial of bevacizumab plus escalated doses of sunitinib in patients with metastatic renal cell carcinoma. J Clin Oncol. 2009;27:1432–9.
25. Hauschild A, Agarwala SS, Trefzer U, Hogg D, Robert C, Hersey P, et al. Results of a phase III, randomized, placebo-controlled study of sorafenib in combination with carboplatin and paclitaxel as second-line treatment in patients with unresectable stage III or stage IV melanoma. J Clin Oncol. 2009;27:2823–30.
26. Azad NS, Posadas EM, Kwitkowski VE, Steinberg SM, Jain L, Annunziata CM, et al. Combination targeted therapy with sorafenib and bevacizumab results in enhanced toxicity and antitumor activity. J Clin Oncol. 2008;26:3709–14.
27. Hecht JR, Mitchell E, Chidiac T, Scroggin C, Hagenstad C, Spigel D, et al. A randomized phase IIIB trial of chemotherapy, bevacizumab, and panitumumab compared with chemotherapy and bevacizumab alone for metastatic colorectal cancer. J Clin Oncol. 2009;27:672–80.
28. O'Brien SG, Guilhot F, Larson RA, Gathmann I, Baccarani M, Cervantes F, et al. Imatinib compared with interferon and low-dose cytarabine for newly diagnosed chronic-phase chronic myeloid leukemia. N Engl J Med. 2003;348:994–1004.
29. Baar J, Silverman P, Lyons J, Fu P, Abdul-Karim F, Ziats N, et al. A vasculature-targeting regimen of preoperative docetaxel with or without bevacizumab for locally advanced breast cancer: impact on angiogenic biomarkers. Clin Cancer Res. 2009;15:3583–90.

Angiogenesis (2012) 15:141–150
DOI 10.1007/s10456-011-9250-0

ORIGINAL PAPER

A phase II study of neoadjuvant bevacizumab plus capecitabine and concomitant radiotherapy in patients with locally advanced rectal cancer

Giampietro Gasparini · Francesco Torino · Takayuki Ueno · Stefano Cascinu · Teresa Troiani · Alberto Ballestrero · Rossana Berardi · Junichi Shishido · Akihiko Yoshizawa · Yukiko Mori · Satoshi Nagayama · Paola Morosini · Masakazu Toi

Received: 25 August 2011 / Accepted: 20 December 2011 / Published online: 3 January 2012

Abstract
Purpose To assess safety and activity of neoadjuvant bevacizumab, capecitabine and standard radiotherapy in locally advanced rectal cancer as well as potential predictive biomarkers.
Patients and methods The multicentric phase II study enrolled 43 patients who received bevacizumab infusion (5 mg/kg) every 2 weeks for 4 cycles; oral capecitabine at 825 mg/m^2 twice a day for 5.5 weeks with external–beam irradiation (50.4 Gy in 28 fractions over 5.5 weeks). We determined certain biomarkers before and after therapy for correlation with response.
Results Post-operative histologic examination revealed no residual cancer cells in 6 of the 43 patients (14%; 95% confidence limits 3.60–24.31%). In another 22 patients (51.2%) a varying percentage of cancer cells in residual areas of fibrosis/ necrosis was found, corresponding to Mandard TRG 2 or 3 classification. Tumor resection with negative circumferential margin was achieved in 38/40 (95%) operated patients. Sphincter–sparing surgery was obtained in 31 (72.1%) patients. Primary tumor and lymph nodes downstaging was observed in 15 (34.9%) and 16 (37.2%) cases, respectively. Neoadjuvant therapy was safe and well tolerated. The most frequent side effects were G1-2 diarrhea, proctitis, rectal bleeding and hypertension. No biomarker tested was significantly predictive of both pathological complete response and disease-free survival. Pre-treatment CD-34 vessel density, post-treatment Ki-67 labeling index and VEGFR-2 cancer cells expression significantly correlated with residual tumor area.
Conclusions The schedule of neoadjuvant therapy tested was safe and active. Pre-treatment vessel density by the panendothelial marker anti CD-34 antibody, post-treatment Ki-67 labeling index and VEGFR-2 expression were significantly associated to residual tumor area. The biomarkers correlations warrant further evaluation in prospective clinical trials.

Keywords Bevacizumab · Capecitabine · Radiotherapy · Rectal cancer · Neoadjuvant-treatment

G. Gasparini (✉) · F. Torino
Unità Operativa Complessa di Oncologia Medica, Azienda Complesso Ospedaliero di Rilevanza Nazionale "S. Filippo Neri", Via G. Martinotti, 20, 00135 Rome, Italy
e-mail: gasparini.oncology@hotmail.it

T. Ueno · J. Shishido · Y. Mori · S. Nagayama · M. Toi
Graduate School of Medicine, Kyoto University, Kyoto, Japan

S. Cascinu · R. Berardi
Oncologia Medica Università delle Marche-Ospedale Umberto I, Ancona, Italy

T. Troiani
Oncologia Medica Università "Federico II", Napoli, Italy

A. Ballestrero
Dipartimento Medicina Interna Università di Genova, Genoa, Italy

A. Yoshizawa
Department of Laboratory Medicine, Shinshu University Hospital, Nagano, Japan

P. Morosini
Medical Affairs-Oncology, Roche S.p.A., Milan, Italy

Introduction

A number of studies and two meta-analyses demonstrated that in locally advanced rectal cancer (LARC) preoperative (neoadjuvant) radiation therapy significantly reduces the

risk of local recurrence and cancer-specific mortality compared to surgery alone [1, 2]. The addition of fluorouracil to radiation therapy significantly increases the rate of pathologic complete response (ypCR) and local control versus radiotherapy alone [3, 4] and chemoradiotherapy is now the standard of neoadjuvant treatment of LARC. The NSABP-R-03 trial compared neoadjuvant versus adjuvant chemoradiotherapy in LARC and demonstrated a significantly improved 5-years disease-free survival (DFS) favoring preoperative therapy, but not showing an overall survival (OS) advantage [5]. The identification of more effective radiation sensitizers represents a topical area of research in such a field. The aim is to improve local control and the possibility of preservation of sphincter function with the hope, ultimately, to avoid the need of abdominal-perineal resection and permanent colostomy, thus improving the quality of life of patients.

Capecitabine is an oral fluoropyrimidine preferentially converted to the active metabolite within tumor cells with higher affinity on the enzyme thymidine phosphorylase [6]. It also showed similar activity compared to infusional fluorouracil when combined with radiotherapy [7].

Oxaliplatin is one of the most active single agents in the treatment of colorectal cancer and it is a potent radiosensitizing drug [8]. However, two recent controlled studies, the Prodiga 2-ACCORD 12/0405 trial and the STAR-01 trial did not demonstrate a statistically significant ypCR rate in the experimental arm with oxaliplatin compared to the standard fluoropyrimidine-based one [9, 10]. Therefore, there was not a real therapeutic progress by using chemotherapy in LARC during the last decade [11].

Among the emerging strategies there are those based on the use of targeted therapies directed against the two more relevant targets in colorectal cancer, namely the epidermal growth factor receptor (EGFR) and vascular endothelial growth factor (VEGF). Phase I–II studies tested cetuximab, an IgG_1 monoclonal antibody anti-EGFR in combination with chemotherapy and radiation therapy as neoadjuvant therapy in LARC [12]. However, in cohorts of unselected patients for K-ras cetuximab did not improve the ypCR rate [13].

More attractive appear the treatments directed to block VEGF. Bevacizumab, the FDA approved anti-VEGF antibody, significantly improved OS in patients with metastatic colorectal cancer when combined with irinotecan-based chemotherapy as first-line therapy [14]. More recently, bevacizumab was tested in the adjuvant setting in two phase III randomized trials in association with oxaliplatin-based chemotherapy. However, both the NSABP C-08 and AVANT studies failed to demonstrate a significant benefit in term of DFS and OS of bevacizumab plus chemotherapy versus chemotherapy alone [15, 16]. Possible explanations for these discordant results in metastatic versus adjuvant settings may be related to the different schedules of chemotherapy used, the possible different biological context concerning the pattern of vascularity of primary tumors versus metastatic lesions and to the duration of administration of bevacizumab [15].

The use of anti-VEGF therapy in LARC is supported by: (1) the radiosensibilization activity demonstrated in experimental models [17] and the in vivo antivascular effects shown in human LARC in the studies performed by Willet et al. [18, 19].

Based on the above rationale it is presumed that LARC is characterized by different tumor biology as compared to radically resected early-stage colorectal cancer. Also the timing and dosing used of neoadjuvant bevacizumab may play a key role favoring its administration in this setting compared to the adjuvant one [15].

We performed the present phase II study in a series of patients affected by LARC in order to verify the toxicity and efficacy of the neoadjuvant schedule of bevacizumab-capecitabine combined with concomitant radiation therapy and to study the role of certain biomarkers in assessing response and outcome of such a therapy.

For the translational study aimed to identify potential predictive biomarkers we evaluated biomarkers related to microvessel density (MVD) and expression of vascular endothelial growth factor receptor-2 (VEGFR-2) as parameters of angiogenesis, tumor associated macrophages (CD68 antibody) apoptosis (M30 antibody), cell kinetics (anti-Ki-67 labeling index), as well as anti-thymidine synthase (TS) and anti-thymidine phosphorylase (TP) being targets of fluoropyrimidines.

Patients and methods

The ML18522 study (NCT01227707; clinicaltrial.gov) was approved by the Ethics Committee at the San Filippo Neri Hospital of Rome and by all the other participating Institutions. Each patient gave his/her written informed consent before being accrued.

Eligibility criteria

Patients >18 years old with histopathologically confirmed rectal adenocarcinoma with the inferior margin within 16 cm from the anal verge as assessed by rectosigmoidoscopy. The tumor had to have evidence of T2 disease with positive locoregional lymph nodes or T3/T4 disease by endorectal ultrasound, computed tomography (CT) and magnetic resonance imaging of the pelvis. Further inclusion criteria were Eastern Cooperative Oncology Group (ECOG) performance status <2 and adequate hematologic, liver and renal functions (neutrophils $\geq 1.5 \times 10^9$/l,

platelet count $\geq 100 \times 10^9$/l; total bilirubin concentration $<1.5 \times$ the upper normal limit (UNL); liver transaminases or alkaline phosphatase concentrations $<2.5 \times$ the UNL; serum creatinine $\leq 1.5 \times$ UNL or creatinine clearance >50 ml/min, urine dipstick of proteinuria $<2+$ or ≤ 1 g of protein in 24 h urine).

Exclusion criteria

Metastatic disease, previous chemotherapy and/or radiation therapy and history of previous other cancers. Patients suffering from the following conditions were also ineligible: inflammatory bowel disease, malabsorption syndrome, uncontrolled hypertension, clinically significant cardiovascular disease (e.g. cerebrovascular stroke or myocardial infarction within 6 months), unstable angina, New York Heart Association (NYHA) grade II or greater congestive heart failure, cardiac arrhythmia requiring medication, bleeding diathesis or coagulopathy, assumption of anticoagulants and drugs known to predispose to gastrointestinal ulceration and psychiatric disorders or psychological disabilities thought to adversely affect treatment compliance. Patients who underwent major surgical procedure, open biopsy, or significant traumatic injury within 4 weeks prior to study treatment start were also excluded. Pregnant or lactating patients and women with childbearing potential who lacked effective contraception were excluded.

Pre-treatment evaluation

Complete history and physical examination with blood pressure, digital rectal examination, colonoscopy with tumor biopsy, endorectal ultrasound, CT and MRI of the pelvis, abdominal CT, and chest X-ray. Complete laboratory tests included full blood counts, blood electrolytes, creatinine, urea, liver transaminases, alkaline phosphatase, total and direct bilirubin, albumin, LDH, International Normalized Ratio (INR), activated partial thromboplastin time (APTT), urine test and dipstick proteinuria. Cardiac activity was investigated by electrocardiography.

Treatment

Radiotherapy

Radiation therapy was performed by conventional fractionation over a period of 5 weeks. The daily fraction dose was 1.8 Gy. A total dose of 45 Gy was given in five fractions per week over a period of 5 weeks. The treated volume included the macroscopic tumor and its potential extensions within the rectum, extending 6 cm above and 4 cm below the tumor margins and extended 3 cm laterally and antero-posteriorly around the macroscopic limits of the tumor, the mesorectum and the perirectal lymph nodes. The anus was not irradiated unless the tumor extended into the anal canal. All the patients received a total dose of 45 Gy in daily fractions of 1.8 Gy (days 1–5/week) calculated at the International Commission of Radiation Units reference point, at the intersection of the central axes of the three or four beams. A boost to the macroscopic tumor with a 2-cm peripheral margin was planned up to 50.4 Gy in further three fractions.

Bevacizumab and capecitabine

Bevacizumab was administered by intravenous infusion at the dose of 5 mg/kg every 2 weeks for 4 courses, with the first infusion given 2 weeks before the concurrent administration of capecitabine and radiation therapy.

Capecitabine was orally administered at the fixed dose of 825 mg/m^2 twice a day (interval about 12 h), within 30 min after the end of a meal, continuously for 5.5 weeks, starting from the first day of radiotherapy (days $1 \rightarrow 38$). The first daily dose was administered approximately 2 h before RT, with the second dose administered 12 h later.

Patients were monitored biweekly regarding history, clinical examination with PS, blood count, INR/APTT and biochemistry, including liver function.

The National Cancer Institute Common Toxicity Criteria, version 3.0, was used to grade toxicity. The schedule of bevacizumab was modified in the event of Grade 2–3 of thrombotic, hemorrhagic, proteinuric, hypertensive and allergic adverse events, as pre-specified in details. The drug was withdrawn in the case a patient experienced Grade 4 toxicity, Grade 3 toxicity not resolved to Grade 1 within 4 weeks, arterial thromboembolic events or gastrointestinal perforation.

The doses of capecitabine were adjusted for adverse events. In brief, in case of capecitabine Grade ≥ 2 toxicity, the drug was interrupted and appropriate symptomatic treatment was administered. When the toxicity resolved to Grade 0–1, treatment was continued at 75% of the original dose in case of the first appearance of the respective toxicity and at 50% of the starting dose in case of the second appearance. In case of Grade 3 toxicity capecitabine was withheld until the toxicity resolved to Grade 0–1, and then continued at 75% of original dose. If radiotherapy caused local Grade ≥ 2 toxicity, it was withheld until toxicity resolved to Grade 0–1, and then restarted with prophylactic treatment. If the same Grade ≥ 2 toxicity recurred, treatment was withheld until the toxicity resolved to Grade 0–1 and the treatment was restarted if clinically necessary with a decreased dose or longer intervals in-between radiation, with a concomitant reduction of the chemotherapy schedule as detailed above.

If toxicity required a dosing delay or interruption of all study drugs for more than 3 weeks, the patient was withdrawn from the study. If capecitabine has to be discontinued permanently due to toxicity, the patient will be allowed to continue only with bevacizumab. If bevacizumab had to be discontinued permanently due to toxicity, the patient will be allowed to continue only with capecitabine.

The relative dose intensity of bevacizumab, capecitabine and RT was calculated as the dose intensity divided by the planned dose intensity × 100.

Surgery

Within 6–8 weeks after completion of neoadjuvant therapy and at least 6 weeks after the last dose of bevacizumab, surgery with total mesorectal excision was performed. Surgery was performed with curative intent with at least a minimal distance of 2 cm between the inferior and superior margin of the tumor and the limit of resection. Assessment of the intended surgical procedure (i.e. whether sphincter preservation was deemed possible or not) was performed by the treating surgeon before start of treatment. If adjacent organs were involved, intraoperative surgery was extended to partial or total resection of adjacent pelvic organs. Resection of metastatic sites evident during surgery was allowed.

Adjuvant chemotherapy

Four to 6 weeks after radical (R0) surgery all patients were candidate to receive adjuvant chemotherapy with bolus and infusional 5-fluouracil plus leucovorin (e.g. De Gramont regimen for 12 courses—6 months of treatment). Adjuvant treatment with bevacizumab (5 mg/m^2 every 14 days) was at the investigator's discretion.

Pathology

The extent of residual tumor in the resected specimen was classified according to the TNM staging system of the American Joint Committee on Cancer/International Union Against Cancer. Residual tumor area (RTA) and fibrosis after preoperative therapy were assessed based on the area of cancer and fibrosis, namely the cancer area/cancer area + fibrosis area. Tumor necrosis area (TNA) was calculated as necrosis area/necrosis area + fibrosis area and was semi-quantitatively evaluated according to a 5-point rectal cancer regression grading (tumor regression grade, TRG) suggested by Mandard et al. [20]. We used for statistical purpose the arbitrary cut-off of 15% of RTA to calculate the correlations with the biomarkers tested. A pathologic complete response was defined as the absence of viable tumor cells both in the primary tumor and lymph nodes (ypT0N0), corresponding to Mandard TRG1. Pathologic assessment was performed by an independent pathologist (AY) blinded to the clinic-pathologic data of the patient.

Translational study of predictive and prognostic biomarkers

The tested biomarkers have been evaluated by immunohistochemical assays according to the manufacturer's instruction: CD31, anti-CD31 antibody (JC70A clone, Dako Cytomation, Denmark); CD34, anti-CD34 antibody (QBend-10 clone, Dako Cytomation, Denmark); CD68, anti-CD68 antibody (Dako Cytomation, Denmark); M30, M30 antibody (Roche, Germany); VEGFR-2, anti-VEGFR-2 antibody (55B11 clone, Cell Signaling, MA); Ki67, anti-Ki67 antibody (Invitrogen, CA); Thymidine synthase (TS), anti-TS antibody (Exalpha Biologicals, MA); Thymidine phosphorylase (TP), anti-TP antibody (Abcam, MA).

Microvessel density was assessed by using two different antibodies: anti-CD31 and anti-CD34. The number of cells positive for CD68 and M30 were counted in five different high power fields (×400) and the average was used for scoring. The labeling index for Ki67 was calculated as the average of Ki67-positive cells/all cancer cells in five different high power fields. The intensity of the staining for VEGFR-2, TP and TS was evaluated separately in cancer cells and stromal cells by comparing the slides stained with immunohistochemistry and those with hematoxilin-eosin and it was estimated on a three-tiered scale, encoded as 0 (absent), 1 (weak), 2 (strong). The score of staining intensity was evaluated by three independent pathologists (AY; YM; SN).

Statistical analysis

The primary end-point of the present phase II study was to determine the ypCR rate after neoadjuvant therapy. Secondary end-points included: toxicity, the safety profile of the neoadjuvant therapy, the sphincter-saving procedure rate, clinical tumor and lymph node regression rate, local control and the disease free survival (DFS). Simon's methods will be used to calculate the sample size. Considering the optimal two stage design for phase II study, with the difference $p1 - p0 = 15\%$ between "standard" chemo-radiation ($p0 = 10\%$) and "new therapy" ($p1 = 25\%$), and fixing error probabilities ($\alpha = 0.05$ and $\beta = 0.20$), the total number of patients to be enrolled was 43. The Chi-square test and Fisher's exact test was used for qualitative parameters. Statistical differences within quantitative parameters was determined by Mann–Whitney's nonparametric test. DFS and local disease free survival (local control) were assessed by using the Kaplan and Meyer's method. Multivariate survival analysis was performed using Cox's proportional hazard ratio. Results were

considered to be statistically significant when $P < 0.05$ (two-sided). Pathological compete response, residual tumor, and tumor necrosis has been analyzed in association with DFS by using the Cox regression approach.

Correlation analysis was performed by the Pearson correlation coefficient and two unpaired groups were compared by the Student's T test. When the correlations between DFS and biomarkers were examined, the Log-rank test and the Cox regression approach were adopted.

Results

Patient characteristics

Forty-three patients have been enrolled at the seven Institutions involved in the study from December 2005 through May 2007. The main characteristics of the patients are listed in Table 1. Three patients had cT4 disease (7%), 14 (32.6%) were staged cT3N0, four patients had cT2, N+ disease (9.3%) and overall, radiological lymph node involvement was detected in 28 (65.1%) patients. A patient had unrecognized metastatic disease and died from progressive disease 14 days after the first dose of bevacizumab (2.3%) and two patients (4.6%) refused surgery. Forty (93%) patients were evaluable for response and 42 (97.7%) for toxicity. All the 43 patients were included in the intent-to-treat analysis. Twenty-four (55.8%) of them received adjuvant chemotherapy.

Efficacy

Central histologic examination of post surgery specimens revealed no residual cancer both at the primary tumor (ypT0 or Mandard TRG 1) and in lymph nodes (ypN0) in 6 out of 43 patient (14% 95% CI 3.60–24.31%). In 22 (51.2%) patients a varying percentage of cancer cells in residual area of fibrosis or necrosis were found, corresponding to ypT1-3 or Mandard TRG 2 or 3. Seven (16.3%) of these patients had ≤10% of cancer cells in fibrosis/necrosis area (Table 2).

Resection with negative circumferential margins was achieved in 38 (95%) out of the 40 resected patients. A T-downstaging (the post-treatment migration of stage from initial T3/4 to ypT1-2) was observed in 15 (34.9%) patients. For 19 patients (44.2%) the T parameter remained stable. Of the 28 patients with imaging detectable lymph node disease at presentation, 16 (37.2%) had N-downstaging (no lymph node disease) post-treatment (Tables 2 and 3).

Three patients (6.9%) developed distant metastases after the neoadjuvant treatment; two underwent surgery. Forty patients (93%) are alive at 16.7 months of median follow-up (range 14–780 days). Eight patients (18.6%) experienced relapse of disease; 5 (11.6%) with local recurrence only; three patients (7%) developed metastatic disease: one in the liver, one in the lung, and the last in both sites. Actuarial 3-years disease-free survival was 75.4% (pCR group 100%, non-pCR group 70.7%; Fig. 1). Sphincter-sparing surgery was achieved in 31 patients (72.1%).

Safety

Most of the adverse events of the neoadjuvant treatment were mild (Grade 1/2; Table 4). There was no Grade 4 or 5 toxicity. Some of the patients experienced Grade 3 toxicities, including diarrhea (3 patients, 7.14%), neutropenia (2 patients), asthenia and hypokalemia (1 patients, respectively). Four (9.52%) patients permanently discontinued treatment due to G3 adverse events, which occurred during the last week of treatment. The most frequent side-effects were: G1/2 diarrhea (12 patients; 28.56%), G1/2 proctitis/proctalgia (9 patients; 21.42%). Hand-foot syndrome (HFS) was mild and transient (only 1 patient with G2 HFS). Bevacizumab-related toxicity included: hypertension in 3 patients (7.14%; G1 = 1 patients; G2 = 2

Table 1 Baseline characteristics of the patients and tumors

Median age (range)	64 years (28–78)	
Gender		
Male	25	58.1%
Female	18	41.9%
P.S. (ECOG)		
0	34	79.1%
1	9	20.9%
cT2,N1,M0	4	9.3
cT3,N0,M0	14	32.56
cT3,N1,M0	20	46.51
cT3,Nx,M0	1	2.33
cT4,N1,M0	1	2.33
cT4,N2,M0	1	2.33
cTX,N2,M0	1	2.33
cT4,N2,M1	1	2.33

Table 2 Overall response to the neoadjuvant treatment

Characteristics ($n = 40$)	No. of patients (%)
Pathologic complete response	6 (14)
Microscopic residual disease (≤15% tumor area/fibrosis-necrosis area)	7 (16.3)
T downstaging	15 (34.9)
N downstaging	18 (41.86)
T stable downsizing	19 (44.2)

Table 3 Migration of stage after the neoadjuvant treatment

Base line	Pts no.	ypT0	ypT1	yPT2	ypT3	ypT4	ypN0	ypN1	ypN2
cT2	4	1	0	2	1	0	–	–	–
cT3	33	5	2	13	13	0	–	–	–
cT4	2	0	0	0	2	0	–	–	–
cTx	1	0	0	0	1	0			
cN0	14	–	–	–	–	–	12	2	0
cN+	25	–	–	–	–	–	18	5	2
cNx	1	–	–	–	–	–	1		
Total	40/43	6	2	15	17	0			

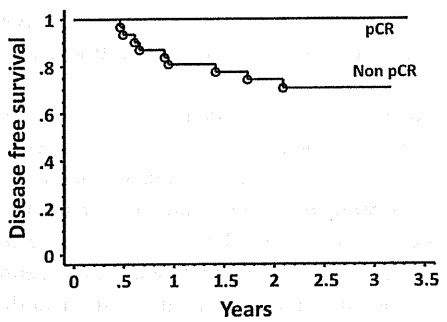

Fig. 1 Disease free survival by response to the treatment (Kaplan-Meier curve)

patients), proteinuria in 1 patient (2.38%; G2), epistaxis in 1 patient (2.3%; G2). No major hemorrhages, thromboembolic events or perforation occurred.

Overall 7 patients experienced serious adverse events, including the death of a patient with progressive disease. One patient died due bowel perforation before receiving adjuvant treatment (1 month after surgery, 81 days after the last dose of bevacizumab). Another patient presented failure to anastomosis (97 days after last bevacizumab) and a patient experienced postoperative abscess (75 days after bevacizumab). Two patients were admitted to hospital due to G3 hypokaliemia and myocardial ischemia, resolved with medical treatment. Only the latter patient was under adjuvant chemotherapy.

Biomarkers of response and prognosis

Biological correlations were performed on 27 biopsy specimens and 38 surgical specimens among the 40 patients evaluable for response with both biopsy and surgical adequate specimens available from 25 patients.

Relationship between biomarkers and clinical outcomes

No significant statistical correlation was observed between ypCR and any biomarker tested. By simple logistic regression model, pre-treatment levels of CD34-positive vessel density were associated with RTA. The patients having tumors with higher density of CD34-positive vessels as compared to those tumors with lower CD34-stained vessels were significantly associated with RTA less than 15% ($P = .0358$; Fig. 2). There was no correlation between treatment response and the pre-treatment levels of all the other markers including CD31-positive vessel density, VEGFR-2 expression both in tumor cells ($P = .42$) and stromal cells ($P = .28$), TP both in tumor cells ($P = .70$) and stroma ($P = .47$), TS both in tumor cells ($P = .99$) and stroma ($P = .99$), CD68 ($P = .60$) and M30 ($P = .30$).

When the correlations between DFS and biomarkers were examined by multiple regression model (log-rank test and Cox regression approach), no biomarker showed a statistically significant correlation with DFS.

When the association between post-treatment levels of each marker and RTA was examined, a statistically significant correlation between post-treatment Ki67 labeling indexes and levels of VEGFR-2 expression in cancer cells was found ($P < .0001$ and $P = .007$, respectively; Figs. 3, 4).

Relationship between pathological response and prognosis

The pathologic response (ypCR, residual tumor, and tumor necrosis) has been analyzed in association with DFS by using the Cox regression approach. Since no event was observed in the ypCR group, neither log-rank test nor the Cox regression analysis gave a result.

When the associations between DFS and RTA, or between DFS and TNA area was evaluated, there was a trend for a correlation between DFS and RTA by the Cox regression analysis ($P = .12$).

Discussion

The seminal translational study by Willet et al. [19] confirmed, for the first time, that bevacizumab exhibits antivascular effects in human rectal cancer by decreasing tumor blood perfusion, microvessel density, the interstitial

Table 4 Main toxicity during the neoadjuvant treatment

Side effect	Total (%)	G1	G2	G3
Abdominal pain	1 (2.38)	1 (2.38)		
Anorectal discomfort	2 (4.76)	1 (2.38)	1 (2.38)	
Constipation	1 (2.38)	1 (2.38)		
Diarrhoea	15 (35.7)	7 (16.66)	5 (11.9)	3 (7.14)
Haemorrhoids	1 (2.38)	1 (2.38)		
Nausea	1 (2.38)	1 (2.38)		
Perianal erythema	1 (2.38)		1 (2.38)	
Proctalgia	5 (11.9)	2 (4.76)	3 (7.14)	
Proctitis	4 (9.52)	2 (4.76)	2 (4.76)	
Rectal haemorrhage	1 (2.38)	1 (2.38)		
Rectal tenesmus	2 (4.76)	2 (4.76)		
Asthenia	4 (9.52)	2 (4.76)	1 (2.38)	1 (2.38)
Fatigue	3 (7.14)	2 (4.76)	1 (2.38)	
Cystitis	3 (7.14)	2 (4.76)	1 (2.38)	
Hyperuricaemia	1 (2.38)	1 (2.38)		
Hypokalaemia	2 (4.76)		1 (2.38)	1 (2.38)
Dysuria	3 (7.14)	2 (4.76)	1 (2.38)	
Proteinuria	1 (2.38)		1 (2.38)	
Haematuria	2 (4.76)		2 (4.76)	
Pollakiuria	1 (2.38)	1 (2.38)		
Strangury	2 (4.76)		2 (4.76)	
Vulvovaginal burning sensation	1 (2.38)		1 (2.38)	
Hypoxia	1 (2.38)	1 (2.38)		
Dermatitis	1 (2.38)	1 (2.38)		
Dermatitis exfoliative	1 (2.38)		1 (2.38)	
Hypertension	3 (7.14)	1 (2.38)	2 (4.76)	
Anaemia	1 (2.38)	1 (2.38)		
Leukopenia	3 (7.14)	2 (4.76)	1 (2.38)	
Neutropenia	6 (14.28)	3 (7.14)	1 (2.38)	2 (4.76)
Epistaxis	1 (2.38)		1 (2.38)	

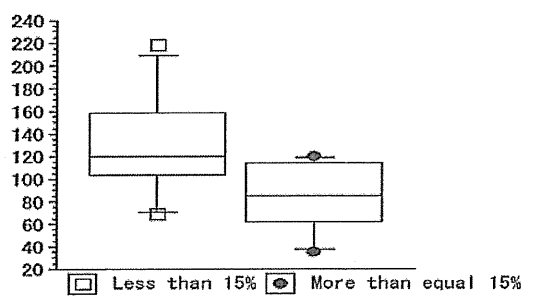

Fig. 2 Using the cut-off value of 15% for residual tumor area, the patients with values <15% showed a statistically significant higher CD-34 vessel staining

fluid pressure and the number of circulating endothelial cells, all these parameters being associated with tumor stabilization or regression.

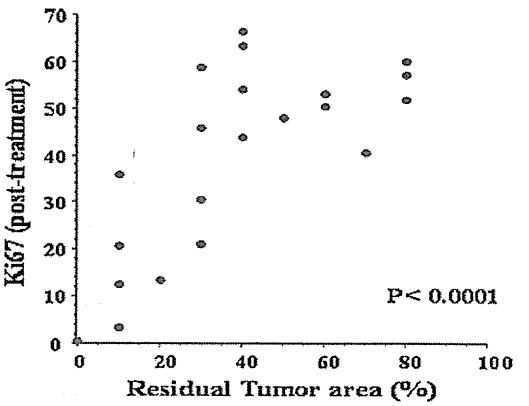

Fig. 3 Correlation between post-treatment Ki67 level and residual tumor area

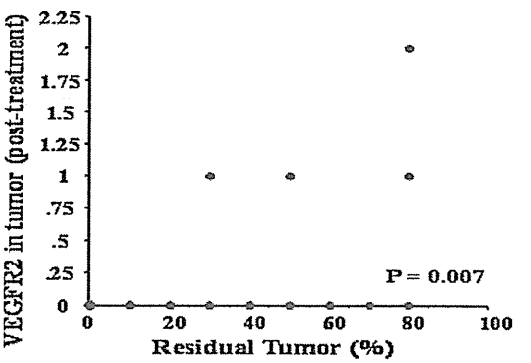

Fig. 4 Correlation between post-treatment tumor VEGFR-2 levels and residual tumor area

A second phase I–II study was performed by Willet et al. [20] to assess the safety and efficacy of neoadjuvant bevacizumab with standard chemoradiotherapy in a cohort of 32 patients with LARC. The Authors demonstrated that all the patients achieved some degree of local response and a ypCR in 5 cases (16%). All the patients underwent a RO resection [20]. When the Authors correlated the changes in biomarkers with treatment outcome they found that VEGFR-1 pretreatment inversely correlated with tumor regression and that circulating VEGF and IL-6 levels predicted enhanced efficacy of the combined therapy.

In the present study histologic examination of postsurgical specimens revealed no residual disease in both the primary tumor and perirectal lymph nodes in 6 of 43 patients. A low percentage of cancer cells was found in the residual area of fibrosis or necrosis in 22 patients (51.2%), corresponding to ypT_{1-3} or Mandard classification TRG 2 or 3, with 7 cases (16.3%) among these patients with ≤15% of cancer cells in fibrosis/necrosis area. During the follow-up 8 patients experienced recurrent disease, 5 of whom with local relapse alone. Sphincter-sparing surgery was achieved in 31 cases (72.1%). Regarding safety, most of

the adverse side effects of the combined neoadjuvant therapy were mild with only 5 patients who experienced Grade 3 toxicity (diarrhea, neutropenia, and hypokalemia).

Similar results have been recently reported by Velenik et al. [21] and by Crane et al. [22] in a small cohort of 25 patients by using a slightly higher dosage of capecitabine and the same schedule of bevacizumab and radiation therapy as in our study. Furthermore, comparable ypCR rates have been obtained in a phase I dose-escalation study by Czito et al. [23] and by Kennecke et al. [24] in a phase II trial, where concurrent oxaliplatin, capecitabine and bevacizumab combined with radiation therapy were evaluated.

Noguè et al. [25] reported the results of a neoadjuvant phase II study with four cycles of oxaliplatin, capecitabine (XELOX regimen) and bevacizumab followed by capecitabine, bevacizumab and concomitant radiation therapy. Using the above intensive therapy the Authors reported a ypCR rate of 36% in 45 evaluable patients.

In a subset of 27 cases we obtained sufficient pre- and post-treatment pathologic material to perform correlations between the biomarkers tested and the efficacy of combined therapy. We used the two panendothelial markers CD31 and CD34 because human vascular endothelium is antigenically heterogeneous [26] and each antibody gives different staining information. In particular, CD31 is a glycoprotein expressed during the differentiation of myelomonocitic cells which is identical to the PECAM-1 molecule present in endothelial cells of blood capillaries and lymphatic microvessels. It is preferentially detected within intercapillary junctions. The expression of CD34, recognizing a transmembrane glycoprotein of 115 kD, is mostly confined to abluminal endothelium microprocesses and may indicate early endothelial cell sprouting and migration [27]. No statistically significant correlation was observed between ypCR and any biomarker tested. Pretreatment levels of CD34 vessel density were significantly associated to RTA. The patients with RTA $\leq$15% showed higher density of CD34-positive vessels as compared to those with larger RTA ($P = .0358$), suggesting that the more vascularized tumors positive for CD34 staining responded better to neoadjuvant treatment. On the contrary, MVD assessed by using the anti-CD31 antibody was not statistically associated to RTA. These different results may be explained by the diverse sensitivity and specificity of the two panendothelial markers used in the identification of endothelial cells within tumor microvessels [28].

We further analyzed the correlation of post-treatment biomarkers and RTA. A significant correlation was observed of Ki-67 labeling index and RTA ($P < .0001$) in agreement with the results by Jacob et al. [29]. It appears plausible that the persistence of a fraction of high-proliferative cells in a larger RTA might be representative of resistant clones of cells and therefore, of a more aggressive phenotype. However, a longer follow up is needed to demonstrate whether the persistence of a variable percentage of high-proliferative cells influences or not either local relapse rate or survival of patients. Furthermore, low levels of VEGFR-2 expression in cancer cells after therapy were associated to RTA ($P = .007$). Zlobec et al. [30] in a cohort of 104 patients with LARC treated with preoperative radiotherapy alone found that the combined analysis of VEGF and EGFR was predictive of ypCR, with the subgroup of cases with VEGF-positive and EGFR-negative tumors being unresponsive to radiation therapy. However, in such a translational study no patient was treated with bevacizumab.

We assessed tumor associated macrophages (TAMs) because of their role in tumor angiogenesis and sensitivity to anticancer treatments [31]. Steidl et al. [32] suggested that the expression of CD68, a pan-macrophages endosomal glycoprotein, is the best biomarker for macrophages. In our study no association between CD68 stained cells and outcome was demonstrated. This may be due to the complex functions of TAMs that comprise phenotypically and functionally different cell subsets in human cancers. In fact, there is in literature conflicting evidence on the correlation of macrophage numbers with response to treatments and prognosis in different tumor types [33]. Furthermore, we evaluated apoptosis using the M30 antibody and we did not observe a significant association of M30 staining with treatment response. However, this negative result may be attributable to the limited number of cases evaluated.

Kocakoya et al. [34] demonstrated in a cohort of 55 patients affected by LARC and treated with neoadjuvant capecitabine and radiotherapy that TP and TS mRNA were induced by therapy in both responders and non-responders. In our study both TP and TS were not predictive of responsiveness in accordance with the study performed by Boskos et al. [35] in patients with LARC treated with preoperative capecitabine and radiotherapy.

In conclusion, the results of this single-arm phase II study show that such a schedule is active and safe. However, the measures of response did not suggest that bevacizumab adds significant improvement of ypCR rate or the long-term local control over standard neoadjuvant fluoropyrimidine-RT schedules.

A number of open questions remain to be elucidated on the optimal use of antiangiogenic agents in combination with chemotherapy and radiation therapy, in particular regarding the optimal timing of delivery of bevacizumab and the key problem to identify predictive biomarkers of activity capable to select the subgroup of patients who are more likely to gain benefit of antiangiogenic therapy [36]. Long-term follow-up studies regarding the impact of such a therapeutic strategy on DFS and OS and regarding

sub-acute, or chronic morbidity of neoadjuvant bevacizumab are needed. Finally, the analysis of the predictive biomarkers tested in our study, by using low-cost and feasible methods, did not reveal any significant association with ypCR.

Acknowledgments The study was supported in part by Roche S.p.A., Italy. We are indebted to the following investigators who participated in the study: Monica Lencioni, Oncologia Medica Ospedale S. Chiara, Pisa; Roberto Murialdo, Dipartimento Medicina Interna Università di Genova; Cristina Granetto, Oncologia Medica, Ospedale S. Croce & Carle, Cuneo; Angelo Martignetti, Dipartimento Oncologia AUSL7, Siena.

References

1. Cammà C, Giunta M, Fiorica F, Pagliaro L, Craxì A, Cottone M (2000) Preoperative radiotherapy for resectable rectal cancer: a meta-analysis. JAMA 284:1008–1015
2. Colorectal Cancer Collaborative Group (2001) Adjuvant radiotherapy for rectal cancer: a systematic overview of 8, 507 patients from 22 randomised trials. Lancet 358:1291–1304
3. Bosset JF, Colette L, Calais G, Mineur L, Maingon P, Radosevic-Jelic L et al (2006) Chemotherapy with preoperative radiotherapy in rectal cancer. N Engl J Med 355:1114–1123
4. Gerard JP, Conroy T, Bonnetain F, Bouché O, Chapet O, Closon-Dejardin MT et al (2006) Preoperative radiotherapy, with or without concurrent 5fluorouracil and leucovorin in T3–T4 rectal cancers: results of the FFCD 9203 trial. J Clin Oncol 24:4620–4625
5. Roh MS, Colangelo LH, O'Connell MJ, Yothers G, Deutsch M, Allegra CJ et al (2009) Preoperative multimodality therapy improves disease-free survival in patients with carcinoma of the rectum: NSABP R-03. J Clin Oncol 27:5124–5130
6. Sawada N, Ishikawa T, Sekiguchi F, Tanaka Y, Ishitsuka H (1999) X-ray irradiation induces thymidine phosphorylase and enhances the efficacy of capecitabine (xeloda) in human cancer xenografts. Clin Cancer Res 5:2948–2953
7. Ben-Josef E (2007) Capecitabine and radiotherapy as neoadjuvant treatment for rectal cancer. Am J Clin Oncol 30:649–655
8. Cividalli A, Ceciarelli F, Livdi E, Altavista P, Cruciani G, Marchetti P et al (2002) Radiosensitization by oxaliplatin in a mouse adenocarcinoma: influence of treatment schedule. Int J Radiat Oncol Biol Phys 52:1092–1098
9. Gérard JP, Azria D, Gourgou-Bourgade S, Martel-Laffay I, Hennequin C, Etienne PL et al (2010) Comparison of two neoadjuvant chemoradiotherapy regimens for locally advanced rectal cancer: results of the phase III trial ACCORD 12/0405-Prodige 2. J Clin Oncol 28:1638–1644
10. Aschele C, Cionini L, Lonardi S, Pinto C, Cordio S, Rosati S et al (2011) Primary tumor response to preoperative chemoradiation with or without oxaliplatin in locally advanced rectal cancer: pathologic results of the STAR-01 randomized Phase III trial. J Clin Oncol 29:2773–2780
11. Weiser MR (2011) Rectal cancer trials: no movement. J Clin Oncol 29:2746–2748
12. Debucquoy A, Machiels JP, McBride WH, Haustermans K (2010) Integration of epidermal growth factor receptor inhibitors with preoperative chemoradiation. Clin Cancer Res 16:2709–2714
13. Rödel C, Arnold D, Hipp M, Liersch T, Dellas K, Iesalnieks I et al (2008) Phase I-II trial of cetuximab, capecitabine, oxaliplatin, and radiotherapy as preoperative treatment in rectal cancer. Int J Radiat Oncol Biol Phys 70:1081–1086
14. Hurwitz HI, Fehrenbacher L, Hainsworth JD, Heim W, Berlin J, Holmgren E et al (2005) Bevacizumab in combination with fluorouracil and leucovorin: an active regimen for first-line metastatic colorectal cancer. J Clin Oncol 23:3502–3508
15. Allegra CJ, Yothers G, O'Connell MJ, Sharif S, Petrelli NJ, Colangelo LH et al (2011) Phase III trial assessing bevacizumab in stages II and III carcinoma of the colon: results of NSABP protocol C-08. J Clin Oncol 29:11–16
16. De Gramont A, Van Cutsem E, Tabernero J, Moore MJ, Cunningham D, Rivera F et al (2011) AVANT: results from a randomized, three-arm multinational phase III study to investigate bevacizumab with either XELOX or FOLFOX4 versus FOLFOX4 alone as adjuvant treatment for colon cancer. J Clin Oncol 29(suppl 4); abstr 362
17. Willett CG, Kozin SV, Duda DG, di Tomaso E, Kozak KR, Boucher Y et al (2006) Combined vascular endothelial growth factor-targeted therapy and radiotherapy for rectal cancer: theory and clinical practice. Semin Oncol 33(Suppl 10):S35–S40
18. Willett CG, Boucher Y, di Tomaso E, Duda DG, Munn LL, Tong RT et al (2004) Direct evidence that the VEGF-specific antibody bevacizumab has antivascular effects in human rectal cancer. Nat Med 10:145–147
19. Willett CG, Duda DG, di Tomaso E, Boucher Y, Ancukiewicz M, Sahani DV et al (2009) Efficacy, safety, and biomarkers of neoadjuvant bevacizumab, radiation therapy, and fluorouracil in rectal cancer: a multidisciplinary phase II study. J Clin Oncol 27:3020–3026
20. Mandard AM, Dalibard F, Mandard JC, Marnay J, Henry-Amar M, Petiot JF et al (1994) Pathologic assessment of tumor regression after preoperative chemoradiotherapy of esophageal carcinoma. Clinicopathologic correlations. Cancer 73:2680–2686
21. Velenik V, Ocvirk J, Music M, Bracko M, Anderluh F, Oblak I et al (2011) Neoadjuvant capecitabine, radiotherapy, and bevacizumab (CRAB) in locally advanced rectal cancer: results of an open-label phase II study. Radiat Oncol 6:105–112
22. Crane CH, Eng C, Feig BW, Das P, Skibber JM, Chang GJ et al (2010) Phase II trial of neoadjuvant bevacizumab, capecitabine, and radiotherapy for locally advanced rectal cancer. Int J Radiat Oncol Biol Phys 76:824–830
23. Czito BG, Bendell JC, Willett CG, Morse MA, Blobe GC, Tyler DS et al (2007) Bevacizumab, oxaliplatin, and capecitabine with radiation therapy in rectal cancer: phase I trial results. Int J Radiat Oncol Biol Phys 68:472–478
24. Kennecke H, Berry S, Wong R, Zhou C, Tankel K, Easaw J et al (2011) Pre-operative bevacizumab, capecitabine, oxaliplatin and radiation among patients with locally advanced or low rectal cancer: a phase II trial. Eur J Cancer (in press)
25. Nogué M, Salud A, Vicente P, Arriví A, Roca JM, Losa F et al (2011) Addition of bevacizumab to XELOX induction therapy plus concomitant capecitabine-based chemoradiotherapy in magnetic resonance imaging-defined poor-prognosis locally advanced rectal cancer: the AVACROSS study. Oncologist 16:614–620
26. Kuzu I, Bicknell R, Harris AL, Jones M, Gatter KC, Mason DY (1992) Heterogeneity of vascular endothelial cells with relevance to diagnosis of vascular tumours. J Clin Pathol 45:143–148
27. Sauter B, Foedinger D, Sterniczky B, Wolff K, Rappersberger K (1998) Immunoelectron microscopic characterization of human dermal lymphatic microvascular endothelial cells. Differential expression of CD31, CD34, and type IV collagen with lymphatic endothelial cells versus blood capillary endothelial cells in normal human skin, lymphangioma, and hemangioma in situ. J Histochem Cytochem 46:165–176

28. Miettinen M, Lindenmayer AE, Chaubal A (1994) Endothelial cell markers CD31, CD34, and BNH9 antibody to H- and Y-antigens—evaluation of their specificity and sensitivity in the diagnosis of vascular tumors and comparison with von Willebrand factor. Mod Pathol 7:82–90
29. Jakob C, Liersch T, Meyer W, Becker H, Baretton GB, Aust DE (2008) Predictive value of Ki67 and p53 in locally advanced rectal cancer: correlation with thymidylate synthase and histopathological tumor regression after neoadjuvant 5-FU-based chemoradiotherapy. World J Gastroenterol 14:1060–1066
30. Zlobec I, Vuong T, Compton CC, Lugli A, Michel RP, Hayashi S et al (2008) Combined analysis of VEGF and EGFR predicts complete tumour response in rectal cancer treated with preoperative radiotherapy. Br J Cancer 98:450–456
31. Jinushi M, Chiba S, Yoshiyama H, Masutomi K, Kinoshita I, Dosaka-Akita H et al (2011) Tumor-associated macrophages regulate tumorigenicity and anticancer drug responses of cancer stem/initiating cells. Proc Natl Acad Sci USA 108:12425–12430
32. Steidl C, Lee T, Shah SP, Farinha P, Han G, Nayar T et al (2010) Tumor-associated macrophages and survival in classic Hodgkin's lymphoma. N Engl J Med 362:875–885
33. Bingle L, Brown NJ, Lewis CE (2002) The role of tumour-associated macrophages in tumour progression: implications for new anticancer therapies. J Pathol 196:254–265
34. Kocakova I, Svoboda M, Kubosova K, Chrenko V, Roubalova E, Krejci E et al (2007) Preoperative radiotherapy and concomitant capecitabine treatment induce thymidylate synthase and thymidine phosphorylase mRNAs in rectal carcinoma. Neoplasma 54:447–453
35. Boskos CS, Liacos C, Korkolis D, Aygerinos K, Lamproglou I, Terpos E et al (2010) Thymidine phosphorylase to dihydropyrimidine dehydrogenase ratio as a predictive factor of response to preoperative chemoradiation with capecitabine in patients with advanced rectal cancer. J Surg Oncol 102:408–412
36. Zhang D, Hedlund E, Lim S, Chen F, Zhang Y, Sun B et al (2011) Antiangiogenic agents significantly improve survival in tumor-bearing mice by increasing tolerance to chemotherapy-induced toxicity. Proc Natl Acad Sci USA 108:4117–4122

Breast Cancer
DOI 10.1007/s12282-012-0363-0

ORIGINAL ARTICLE

Photoacoustic mammography: initial clinical results

Toshiyuki Kitai · Masae Torii · Tomoharu Sugie · Shotaro Kanao · Yoshiki Mikami · Tsuyoshi Shiina · Masakazu Toi

Received: 12 December 2011 / Accepted: 12 March 2012

Abstract
Purpose Photoacoustic tomography can image the hemoglobin distribution and oxygenation state inside tissue with high spatial resolution. The purpose of this study is to investigate its clinical usefulness for diagnosis of breast cancer and evaluation of therapeutic response in relation to other diagnostic modalities.
Materials and methods Using a prototype machine for photoacoustic mammography (PAM), 27 breast tumor lesions, including 21 invasive breast cancer (IBC), five ductal carcinoma in situ (DCIS), and one phyllodes tumor, were measured. Nine out of twenty-one IBC patients had received primary systemic therapy (PST).
Results Eight out of twelve IBC without PST were visible. Notably, detection was possible in all five cases with DCIS, whereas it was not in one case with phyllodes tumor. Seven out of nine IBC with PST were assigned as visible in spite of decreased size of tumor after PST. The mean value of hemoglobin saturation in the visible lesions was 78.6 %, and hemoglobin concentration was 207 μM. The tumor images of PAM were comparable to those of magnetic resonance imaging (MRI).
Conclusions It is suggested that PAM can image tumor vascularity and oxygenation, which may be useful for diagnosis and characterization of breast cancer.

Keywords Photoacoustic mammography · Optical imaging · Near-infrared · Breast cancer · Tumor vascularity · Oxygenation

T. Kitai (✉) · M. Torii · T. Sugie · M. Toi
Department of Breast Surgery, Graduate School of Medicine, Kyoto University, 54 Kawaracho Shogoin Sakyoku, Kyoto 6068507, Japan
e-mail: kitait@kuhp.kyoto-u.ac.jp

S. Kanao
Department of Diagnostic Imaging and Nuclear Medicine, Graduate School of Medicine, Kyoto University, Kyoto, Japan

Y. Mikami
Department of Diagnostic Pathology, Graduate School of Medicine, Kyoto University, Kyoto, Japan

T. Shiina
Department of Human Health Science, Graduate School of Medicine, Kyoto University, Kyoto, Japan

Introduction

Breast cancer is one of the most common malignant diseases in women. Early detection and diagnosis are essential to decrease mortality. In addition, as the number of cases of primary systemic therapy (PST) increases, efforts have been made to develop a sensitive method for monitoring treatment effect [1–3]. Conventional diagnostic modalities, including X-ray mammography (MMG), ultrasonography (US), and magnetic resonance imaging (MRI), are useful for these purposes, but each has some drawbacks. Mammography is associated with ionizing radiation and has diagnostic weakness for dense breast. The results of ultrasound greatly depend on the instrumental performance and examiner's skill. MRI requires use of contrast medium, which is not suitable for mass screening and repeated examination.

Optical detection of breast cancer using near-infrared (NIR) light has drawn much attention because it can measure the hemoglobin distribution and oxygenation state inside the tissue noninvasively [4, 5]. Angiogenesis is essential for breast cancer growth and also correlates with the malignant potential of precursor lesion [6–9]. It is known that microvessel density in cancer tissue

Published online: 07 April 2012

significantly decreases in responders to PST from the early period [10]. Therefore, optical imaging has great potential as the basis for novel diagnostic modalities for breast cancer. Several studies have reported promising results for diffuse optical tomography (DOT) used for differential diagnosis and therapeutic monitoring of breast cancer [11–17]. However, at present, its clinical usefulness seems to be limited due to poor spatial resolution. Photoacoustic tomography is another modality of optical imaging based on photoacoustic technology, enabling imaging of the hemoglobin distribution and oxygenation state inside tissue with higher spatial resolution than DOT [18–20]. There are a few preliminary reports on such approaches for breast cancer [21–23].

In this paper, we report early results of clinical application of photoacoustic mammography (PAM) and investigate its usefulness for diagnosis of breast cancer and evaluation of therapeutic response in relation to other diagnostic modalities.

Materials and methods

Instruments

A prototype machine of a dual illuminated mode photoacoustic tomography system (Canon Inc., Tokyo, Japan) was used [24, 25]. Figure 1 shows a photograph of the machine and a schematic of the measurement. The patient–instrument interface was a sliding bed with a 17 cm × 18 cm hole, which was mounted on a frame housing the laser-emitting and ultrasound detection units. The patient lies in prone position on the bed with her breast placed in the hole. The breast is mildly compressed in craniocaudal direction between holding plates. Acoustic coupling gel is used between the breast and the holding plate that carries the scanning system. Pulsed laser beams irradiate the breast from both sides, and photoacoustic signals are detected on the caudal side by an array transducer. The lasers are mounted at the bottom of the bed and coupled to the scanning system. A Ti:Sa laser optically pumped with a Q-switched Nd:YAG laser is used, having a tunable wavelength in the range 700–900 nm. The measurable area was 30 mm × 46 mm for one scan, which took 45 s. In the first 16 cases, the scan was performed at three adjacent areas where the lesion was considered to be located in the diseased breast and one area in the intact breast. In the last 15 cases, the scanning system was automatically moved in an area of 120 mm × 46 mm. Specific parameters of the PAM were as follows:

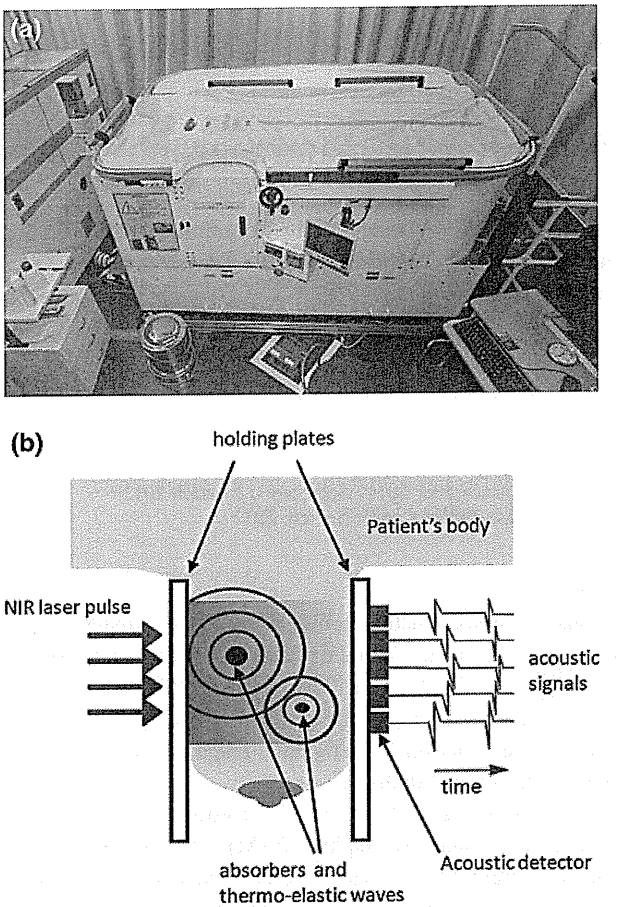

Fig. 1 **a** The prototype machine. The patient–instrument interface was a sliding bed with a 17 cm × 18 cm hole. The lasers are mounted at the bottom of the bed and coupled to the ultrasound scanning system. **b** Schematic of the PAM measurement: a near-infrared laser pulse irradiates the breast, and thermoelastic waves produced by absorbers in the breast are detected by ultrasound detectors

Laser	
Wavelengths	1064, 825, 797, 756 nm
Pulse width	7 ns
Repetition rate	10 Hz
Detector	
Matrix shape	Rectangular
Number of elements	15 by 23
Element size	2 × 2 mm
Central frequency	1 MHz

Photoacoustic image reconstruction was carried out using a modified universal backprojection algorithm. Assuming that the breast consisted of homogeneous tissue

with known μ_a and μ_s', the μ_a values of the absorbers were calculated from the initial pressure rise after the laser pulse using the equation shown below [4]. The light fluence distribution inside the breast was estimated using the published data of absorption and scattering coefficients (μ_a and μ_s') of the breast corresponding to the patient's age [26].

$$p_0 = \Gamma \eta_{th} \mu_a F,$$

where p_0 is the initial pressure after the laser pulse and Γ is the Grueneisen parameter; at body temperature, $\Gamma = 0.20$. η_{th} is the percentage that is converted to heat, μ_a is the absorption coefficient, and F is the light fluence

Thus, the distribution of μ_a in the breast can be calculated from the initial pressure distribution at each wavelength. The oxygen saturation of hemoglobin (SO_2) and total hemoglobin concentration (THC) of the lesions were calculated using the μ_a values at 797 and 756 nm. Extinction coefficients of oxyhemoglobin and deoxyhemoglobin of 0.231 and 0.259 at 797 nm, and 0.163 and 0.511 at 756 nm, respectively, were used.

Patients

Thirty-one patients who were histologically diagnosed with breast cancer or phyllodes tumor were recruited in this study at Kyoto University Hospital from August 2010 to July 2011. Twenty-seven breast lesions of twenty-six cases were subjected to analysis. The other five cases were excluded from analysis because the tumor was outside the measurable area of PAM as the breast was too small or the tumor was located very near to chest wall. MMG, US, and MRI were undertaken as routine preoperative workup. All patients underwent breast surgeries following PAM measurements within 1 month, and no anticancer treatment was given during the interval. The excised specimens were pathologically examined. For assignment of the pathological effect of PST, the Histopathological Criteria for Assessment of Therapeutic Response of the Japanese Breast Cancer Society were used [27], which assign the pathological effect as grade 0 (no response) to grade 3 (complete response). Visibility of PAM imaging was assigned by one of the authors who is a radiologist specialized in diagnosis of breast cancer. Our procedures were as follows: Signals which were supposed to come from vascular-rich lesions or vessels were extracted from PAM images without considering clinical data including other imaging modalities. The selection criteria were the intensity and morphology of the signal. Linear, winding, or branched shaped signals were attributed to vessels. Grouped or locally scattered signals were attributed to the vascular-rich lesion. Usually, several signals or groups were extracted from one breast measurement. Each PAM signal was then correlated with that of MRI by comparing the locations. The assignment of the location was adjusted by the shape of subcutaneous veins which were demonstrated by both PAM and MRI. When any signal was found to be located at the site of the known tumor, the radiologist judged whether the signal was associated with the tumor, considering the intensity, shape, and distribution.

The study protocol was approved by the Medical Ethical Committee of Kyoto University.

Results

The average age was 58.0 years (36–83 years), and the tumor size measured by MRI was 20.1 mm (11–70 mm). Preoperative diagnosis was invasive breast cancer (IBC) in twenty-one breasts, including twenty invasive ductal carcinomas (IDC), one invasive lobular carcinoma (ILC), ductal carcinoma in situ (DCIS) in five cases, and phyllodes tumor in one case. Biological subtype of IBC was estrogen receptor (ER)+/human epidermal growth factor receptor 2 (HER2)− in eighteen lesions, ER−/HER2+ in two, and ER−/HER2− in one. PST was given in 9 out of 21 IBC patients.

The tumor was assigned as visible by PAM in 20 out of 27 breasts (74 %), as shown in Table 1. Table 2 presents the results of IBC cases without PST. Eight out of twelve IBC were visible. Table 3 shows the results with PST. Five out of nine cases showed clinical partial response and pathological therapeutic effect better than grade 2 (marked response). Seven cases were assigned as visible in spite of decreased tumor size after PST. Table 4 presents the results of DCIS and phyllodes tumor. Notably, detection was possible in all five cases with DCIS. On the other hand, it was not possible with phyllodes tumor. Mean SO_2 in the visible lesions was 78.6 % (53.7–100 %), and mean THC was 207 μM (87–309 μM).

Two particular cases of IBC with or without PST are now presented in detail.

Table 1 Tumor visibility on PAM imaging

Diagnosis	Tumor visibility
IBC without PST	8/12
IBC after PST	7/9
DCIS	5/5
Phyllodes tumor	0/1
All	20/27

IBC invasive breast cancer, *PST* preoperative systemic treatment, *DCIS* ductal carcinoma in situ

Table 2 Results in cases of IBC without PST

Case	Diameter (MRI)	Diameter (specimen)	Pathological diagnosis	Subtype	Histological grade	Ki-67	PAM visibility
1	15 mm	17 mm	ILC	ER+/HER2−	2	<5	Yes
2	28	21	IDC	ER+/HER2−	2	10	No
3	19	18	IDC	ER+/HER2−	2	10	Yes
4	13	24	IDC	ER+/HER2−	1	<5	Yes
5	33	24	IDC	ER+/HER2−	1	20	No
6	15	13	IDC + DCIS, high grade	ER−/HER2+	3	20	Yes
7	22	18	IDC	ER+/HER2−	2	15	Yes
8	ND	19	IDC	ER+/HER2−	1	<5	No
9	23	21	IDC	ER+/HER2−	2	3	Yes
10	22	22	IDC	ER+/HER2−	2	27	Yes
11	30	40	IDC	ER+/HER2−	3	40	No
12	19	15	IDC	ER+/HER2−	1	4	Yes

ND not detectable, *IDC* invasive ductal carcinoma, *ILC* invasive lobular carcinoma, *DCIS* ductal carcinoma in situ, *ER* estrogen receptor, *HER2* human epidermal growth factor receptor 2

Table 3 Results in cases of IBC after PST

Case	Subtype	Regimen	Clinical response	Diameter (MRI)	Pathological response	Diameter (specimen)	PAM visibility
1	ER+/HER2−	Let	SD	9 mm	Grade 1a	10 mm	Yes
2	ER+/HER2−	Let + CPA	PR	16, 14	Grade 1b–2a	8, 13	Yes
3	ER+/HER2−	Let + CPA	SD (near PR)	19	Grade 1a	42	No
4	ER+/HER2−	Let + CPA	SD	8	Grade 2a	6	Yes
5	ER+/HER2−	LHRHa + Tam + 5FU	SD	22	Grade 1b	24	Yes
6	ER−/HER2+	FEC > D + H	PR (near CR)	5	Grade 2a	11	No
7	ER+/HER2−	TC	PR	25	Grade 2a	35	Yes
8	ER−/HER2−	TP > FEC	PR	17	Grade 2a	11	Yes
9	ER+/HER2−	AP	PR	4	Grade 3[a]	0	Yes

Grade 1a: mild response. Mild changes in cancer cells regardless of the extent, and/or marked changes in less than 1/3 cancer cells. Grade 1b: moderate response. Marked changes in 1/3–2/3 cancer cells. Grade 2a: high grade changes. Marked changes in more than 2/3 tumor cells with apparent remaining cancer cells. Grade 3: complete response. Necrosis and/or disappearance of all tumor cells, and/or replacement of cancer cells by granulation and/or fibrosis

ER estrogen receptor, *HER2* human epidermal growth factor receptor 2, *Let* letrozole, *CPA* cyclophosphamide, *FEC* epirubicin + 5-fluorouracil (5-FU) + cyclophosphamide, *D* docetaxel, *H* herceptin, *TC* docetaxel + cyclophosphamide, *LHRHa* luteinizing hormone-releasing hormone agonist, *Tam* tamoxifen, *TP* docetaxel + cisplatin, *AP* adriamycin + cisplatin, *SD* stable disease, *PR* partial response, *CR* complete response

[a] DCIS remained

1. IBC without PST

The patient was a 75-year-old woman with left breast cancer. MRI showed a tumor with ring enhancement with diameter of 22 mm. Pathological diagnosis was IDC (ER+/HER2+). At PAM measurement, the breast was compressed to thickness of 58 mm. Figure 2 shows subcutaneous blood vessels by PAM. The value of SO_2 ranged from 92.1 to 98.6 %. Figure 3 shows a maximum-intensity projection (MIP) image of PAM at depth between 7.75 and 11.5 mm, indicating clustered signals aligned in a ring

Table 4 Results in cases of DCIS and phyllodes tumor

Case	Diameter (MRI)	Diameter (specimen)	Pathological diagnosis	PAM visibility
1	30 mm	30 mm	DCIS, intermediate–high grade	Yes
2	11	11	DCIS, high grade	Yes
3	36	45	DCIS, intermediate grade	Yes
4	60	60	DCIS, high grade	Yes
5	70	63	DCIS, low grade	Yes
6	21	35	Phyllodes tumor, border line	No

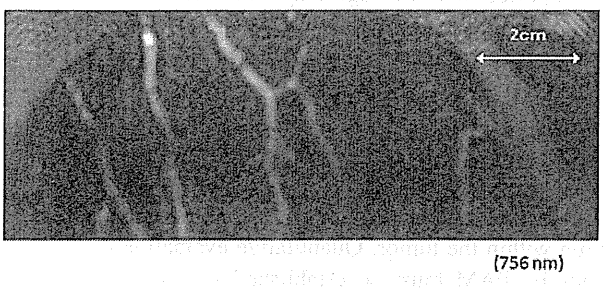

Fig. 2 Subcutaneous blood vessels were clearly shown (depth 1.5–2.25 mm). SO_2 values ranged from 92.1 to 98.6 %

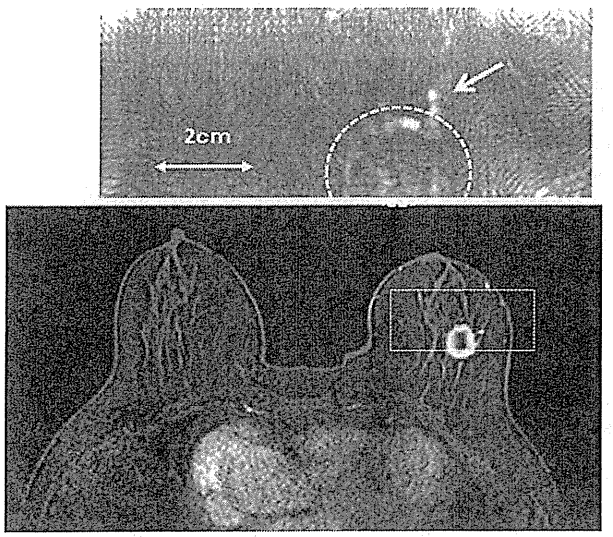

Fig. 3 IBC without PST. *Upper panel* PAM image showed clustered signals aligned in a ring (*dotted circle*) and a linear signal (*arrow*) (depth 7.75–11.5 mm, breast thickness 58 mm). These signals were considered to represent the tumor and the feeding vessel, respectively. Mean values of SO_2 and THC of the tumor were 87.1 % and 112 μM, respectively. *Lower panel* MRI showed a tumor with ring enhancement. The *dotted square* corresponds to the area of the PAM image

shape and a linear-shaped signal. These signals were comparable to the MRI findings and considered to represent the tumor and the feeding vessel, respectively. Mean values of SO_2 and THC in the areas with these signals were 87.1 % and 112 μM, respectively.

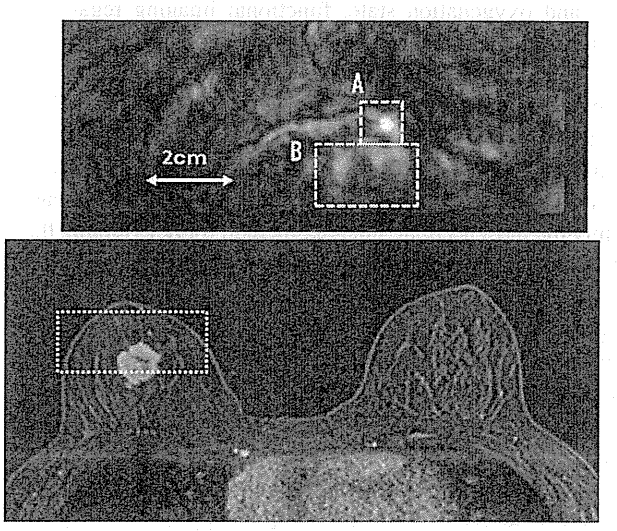

Fig. 4 IBC after PST. *Upper panel* PAM image showed clustered signals (squared areas *A* and *B*) (depth 28.25 mm, breast thickness 68 mm). Areas A and B were assigned as peripheral part and central part of the tumor, respectively. Mean values of SO_2 and THC of the assigned lesions were A: 74.5 % and 385 μM, and B: 53.8 % and 307 μM, respectively. *Lower panel* MRI showed an enhanced tumor of 22 mm size. The *dotted square* corresponds to the area of the PAM image

2. IBC after PST

The patient was a 41-year-old woman with right breast cancer. The tumor was reduced in size from 34 to 22 mm in diameter after 6-month treatment with endocrine therapy. PAM image at depth of 28.25 mm showed signals comparable to those of MRI image (Fig. 4). Pathological diagnosis was IDC (ER+/HER2−), and the therapeutic effect was assigned as grade 1b (moderate response). Mean values of SO_2 and THC of the two assigned lesions were 74.5 % and 385 μM in area A, and 53.8 % and 307 μM in area B, respectively.

Discussion

Photoacoustic tomography refers to imaging that is based on the photoacoustic effect [4, 18–20]. When light is

emitted into tissue, some of the light is absorbed by the object and partially converted into heat. This heat is then further converted to a pressure rise via thermoelastic expansion. The pressure rise is propagated as an ultrasonic wave, which is detected by ultrasonic transducers and used by a computer to form an image. The purpose of using photoacoustic tomography is to combine the contrast of optical absorption with the spatial resolution of ultrasound for deep imaging of living tissue. Since optical absorption provides biological information about tissue vascularization and oxygenation state, functional imaging regarding tissue oxygenation can be obtained. Previous reports using animal models showed successful results of imaging of lymphovascular structure inside tissue [20, 28, 29]. This technology has already been applied to breast cancer patients [21, 23], but the clinical evaluation was limited.

We compared PAM images with MRI, since MRI is currently the most accurate imaging method for determining the extent of disease in the breast [30, 31]. As shown in Figs. 3 and 4, the PAM tumor image was comparable to that of MRI, demonstrating rim enhancement. These findings could be attributable to the distribution of higher vascular densities in the peripheral area of cancer. However, the PAM tumor image was not mass-forming as shown by MRI. Discrepancy in the image presentation probably arises from the difference in distribution of contrast materials. Photoacoustic imaging represents the distribution of hemoglobin inside the vessels, whereas MRI imaging presents not only the tumor vessels but also the surrounding stroma where the contrast media is shed out from the vessels. In a preliminary study using animals and excised breast cancer specimens, the PAM signal intensity was correlated with the microvessel density in the tumor tissue (data not shown).

In this study, 20 out of 27 breast cancer lesions were assigned as visible in PAM images. The detection rate seems acceptable, considering the variety of cases in this series. Previous clinical studies reported PAM images of breast cancer corresponding to the findings of MMG or US [21, 23] and detection rate similar to ours [23], but the patient population was rather homogeneous. This study evaluated PAM images in cases of DCIS and IDC with PST as well. Reasons for failure in unsuccessful cases of IBC without PST were mostly due to small breast size, breast surface deformity, and poor tumor vascularity.

Five cases of DCIS with diameters of 63 and 11 mm were visible by PAM, but phyllodes tumor with diameter of 35 mm was not. These results suggest that PAM may be useful to differentiate malignant lesions from benign ones and also to detect breast cancer at an early stage. It was reported that microvascular density increased at the stage of noninvasive carcinoma [7, 9]. Previous studies of DOT also showed that tissue hemoglobin concentration was a good parameter to differentiate between malignant and benign lesions [15, 17]. High spatial resolution of PAM would be beneficial for detection of small DCIS lesions. Further study is necessary to confirm these hypotheses.

Seven out of nine cases after PST could be detected by PAM in spite of decreased tumor diameter and cellularity. As the number of cases of PST increases, sensitive measures for monitoring therapeutic effect are required [32–35]. As well as radiological imaging modalities and biological markers of biopsy specimens, promising results have been reported for optical imaging using DOT. It has been reported that hemoglobin concentration decreased during PST before morphological changes appeared and that oxygen saturation transiently increased shortly after the start of PST [12, 16]. Since repeated examinations along the treatment course are necessary, the noninvasiveness of optical imaging is beneficial. In addition, PAM has the possibility to monitor not only changes in hemoglobin in the whole tumor but also changes at higher resolution within the tumor. Quantitative evaluation of tumor images by PAM must be established for the purpose of monitoring the effect of PST.

This study used multiple wavelengths to measure PAM signals to estimate the tumor SO_2 and THC, which was the first attempt of its kind in clinical studies. It has been reported that malignant tumor has higher THC and lower SO_2 than background breast tissue. According to a review paper on DOT [17], tumor showed THC of 65 ± 34 μM, being 2.0–4.5-fold higher than the background THC. The tumor SO_2 was 66 ± 24 %, which was 0.8–0.82-fold that of the background SO_2. The values of THC and SO_2 of 207 μM and 78.6 %, respectively, in breast cancer calculated in this study were higher than the reported data of DOT. These discrepancies are partly due to the difference in spatial resolution between the two imaging modalities. Contrast of the tumor arises from the difference of hemoglobin concentration between tumor and normal breast tissues in both PAM and DOT. PAM may select a more confined area where the tissue is more vascular rich and oxygenated than the area defined by DOT. However, there are several problems in quantitative evaluation of SO_2 and THC by PAM: (1) The light distribution in the breast tissue at each wavelength should be known a priori. We used μ_a and μ_s' values reported in past literature to calculate the light distribution, but some deviation from the actual distribution might exist in each case. (2) The direction of the vessels and the shape of absorbers should affect the intensity of PAM signals. (3) Noise occurring at the margin of the breast and the boundaries of the compression plates prevents quantitative measurement of the initial pressure of thermoelastic wave. Noise reduction is essential for quantitative evaluation of optical parameters. Further study is necessary to quantify these optical parameters for clinical use.

Breast compression is an inevitable problem with the present method. We compressed the breast for two reasons: to make contact with the plate carrying the ultrasound detectors and to increase the light fluence rate inside the breast by decreasing the breast thickness. However, compression at high pressure may disturb tissue circulation [36]. Care was taken to apply minimal pressure so as not to change the tissue circulation and oxygenation. In fact, clear demonstration of subcutaneous vasculature and reasonable SO_2 values suggested that the tissue circulation was fairly well maintained.

PAM could provide images of tumor vasculature and oxygenation, which cannot be obtained by MMG or US. However, imaging depth and resolution still require improvement. At present, PAM has an advantage in terms of functional features rather than morphology. The combination of PAM with US, as demonstrated in animal models [24, 25], would be useful to achieve more comprehensive imaging of breast cancer, where the biological and anatomical aspects can be assessed simultaneously. It is suggested that PAM may be useful for diagnosis and characterization of breast cancer, and its further clinical exploration is promising.

Acknowledgments This work is partly supported by the Innovative Techno-Hub for Integrated Medical Bio-imaging Project of the Special Coordination Funds for Promoting Science and Technology, from the Ministry of Education, Culture, Sports, Science, and Technology, Japan.

References

1. Smith PA, D'Orsi C, Newell MS. Screening for breast cancer. In: Harris JR, Lippman ME, Morrow M, Osborne CK, editors. Disease of the breast. 4th ed. Philadelphia: Lippincott–Williams and Wilkins; 2010. pp 87–115.
2. Gounaris I, Provenzano E, Vallier AL, Hiller L, Iddawela M, Hilborne S, et al. Accuracy of unidimensional and volumetric ultrasound measurements in predicting good pathological response to neoadjuvant chemotherapy in breast cancer patients. Breast Cancer Res Treat. 2011;127:459–69.
3. Chen JH, Feig BA, Hsiang DJ, Butler JA, Mehta RS, Bahri S, et al. Impact of MRI-evaluated neoadjuvant chemotherapy response on change of surgical recommendation in breast cancer. Ann Surg. 2009;249:448–54.
4. Wang LV, Wu HI. Biomedical optics principles and imaging. Hoboken: Wiley-Interscience; 2007.
5. Frangioni JV. New technologies for human cancer imaging. J Clin Oncol. 2008;26:4012–21.
6. Brem SS, Jensen HM, Guillino PM. Angiogenesis as a marker of preneoplastic lesions of the human breast. Cancer. 1978;41:239–44.
7. Viacava P, Naccarato AG, Bocci G, Fanelli G, Aretini P, Lonobile A, et al. Angiogenesis and VEGF expression in pre-invasive lesions of the human breast. J Pathol. 2004;204:140–6.
8. Uzzan B, Nicolas P, Cucherat M, Perret GY. Microvessel density as a prognostic factor in women with breast cancer: a systematic review of the literature and meta-analysis. Cancer Res. 2004;64:2941–55.
9. Guidi AJ, Fischer L, Harris JR, Schnitt SJ. Microvessel density and distribution in ductal carcinoma in situ of the breast. J Natl Cancer Inst. 1994;86:614–9.
10. Makris A, Powles TJ, Kakolyris S, Dowsett M, Ashley SE, Harris AL. Reduction in angiogenesis after neoadjuvant chemoendocrine therapy in patients with operable breast carcinoma. Cancer. 1999;85:1996–2000.
11. Jiang S, Pogue BW, Carpenter CN, Poplack SP, Wells WA, Kogel CA, et al. Evaluation of breast tumor response to neoadjuvant chemotherapy with tomographic diffuse optical spectroscopy: case studies of tumor region-of-interest changes. Radiology. 2009;252:551–60.
12. Soliman H, Gunasekara A, Rycroft M, Zubovits J, Dent R, Spayne J, et al. Functional imaging using diffuse optical spectroscopy of neoadjuvant chemotherapy response in woman with locally advanced breast cancer. Clin Cancer Res. 2010;16:2605–14.
13. Zhu Q, Hegde PU, Ricci A, Kane M, Cronin EB, Ardeshirpour Y, et al. Early-stage invasive breast cancers: Potential role of optical tomography with US localization in assisting diagnosis. Radiology. 2010;256:367–78.
14. Tromberg BJ, Pogue BW, Paulsen KD, Yodh AG, Boas DA, Cerussi AE. Assessing the future of diffuse optical imaging technique for breast cancer management. Med Phys. 2008;35:2443–51.
15. Choe R, Konecky SD, Corlu A, Lee K, Durduran T, Busch DR, et al. Differentiation of benign and malignant breast tumors by in vivo three-dimensional parallel-plate diffuse optical tomography. J Biomed Opt. 2009;14:024020.
16. Roblyer DM, Ueda S, Cerussi AE, Tanamai W, Durkin A, Mehta RS, et al. Oxyhemoglobin flare after the first day of neoadjuvant breast cancer chemotherapy predicts overall response. Cancer Res. 2010;70:363s.
17. Leff DR, Warren OJ, Enfield LC, Hebden J, Yang GZ, Darzi A. Diffuse optical imaging of the healthy and diseased breast: a systematic review. Breast Cancer Res Treat. 2008;108:9–22.
18. Emelianov S, Li P-C, O'Donnell M. Photoacoustics for molecular imaging and therapy. Phys Today. 2009;62:34–9.
19. Laufer J, Delpy D, Elwell C, Beard P. Quantitative spatially resolved measurement of tumor chromophore concentrations using photoacoustic spectroscopy: application to the measurement of blood oxygenation and hemoglobin concentration. Phys Med Biol. 2007;52:141–68.
20. Zhang EZ, Laufer JG, Pedley RB, Beard PC. In vivo high-resolution 3D photoacoustic imaging of superficial vascular anatomy. Phys Med Biol. 2009;54:1035–46.
21. Manohar S, Vaartjes SE, Hespen JCG, Klasse JM, Engh FM, Steenbergen W, et al. Initial results of in vivo non-invasive cancer imaging in the human breast using near-infrared photoacoustics. Opt Exp. 2007;15:12277–85.
22. Kruger RA, Lam RB, Reinecke DR, Del Rio SP, Doyle RP. Photoacoustic angiography of the breast. Med Phys. 2010;37:6096–100.
23. Ermilov SA, Khamapirad T, Conjusteau A, Leonard MH, Lacewell R, Mehta K, et al. Laser optoacoustic imaging system for detection of breast cancer. J Biomed Opt. 2009;14:024007.
24. Fukutani K, Someda Y, Taku M, Asao Y, Kobayashi S, Yagi T, et al. Characterization of photoacoustic tomography system with dual illumination. Proc SPIE 2011;7899:78992J.
25. Tanji K, Watanabe K, Fukutani K, Asao Y, Yagi T. Yamakawa M, et al. Advanced model-based reconstruction algorithm for practical three-dimensional photo acoustic imaging. Proc SPIE 2011;7899:78992K.
26. Suzuki K, Yamashita Y, Ohta K, Kaneko M, Yoshida M, Chance B. Quantitative measurement of optical parameters in normal breasts using time-resolved spectroscopy in vivo results of 30 Japanese women. J Biomed Opt. 1996;1:330–4.

27. Kurosumi M, Akashi-Tanaka S, Akiyama F, Komoike Y, Mukai H, Nakamura S, et al. Histopathological criteria for assessment of therapeutic response in breast cancer (2007 version). Breast Cancer. 2008;15:5–7.
28. Kim C, Song KH, Gao F, Wang LV. Sentinel lymph nodes and lymphatic vessels: noninvasive dual-modality in vivo mapping by using indocyanine green in rats—volumetric spectroscopic photoacoustic imaging and planer fluorescence imaging. Radiology. 2010;255:442–50.
29. Erpelding TN, Kim C, Pramanik M, Jankovic L, Maslov K, Guo Z, et al. Sentinel lymph nodes in the rat: noninvasive photoacoustic and US imaging with a clinical US system. Radiology. 2010;256:102–10.
30. Orel SG, Schnall MD. MR imaging of the breast for the detection, diagnosis, and staging of breast cancer. Radiology. 2001;220:13–30.
31. Tse GM, Chaiwun B, Won KT, Yeung DK, Pang AL, Tang AP, et al. Magnetic resonance imaging of breast lesions: a pathological correlation. Breast Cancer Res Treat. 2007;103:1–10.
32. Chuah BY, Putti T, Salto-Tellez M, Charlton A, Iau P, Buhari SA, et al. Serial changes in the expression of breast cancer-related proteins in response to neoadjuvant chemotherapy. Ann Oncol. 2011;22:1748–54.
33. Smith IE, Dowsett M, Ebbs SR, Dixon JM, Skene A, Blohmer YU, et al. Neoadjuvant treatment of postmenopausal breast cancer with anastrozole, tamoxifen, or both in combination: the immediate preoperative anastrozole, tamoxifen, or combined with tamoxifen (IMPACT) multicenter double-blind randomized trial. J Clin Oncol. 2005;23:5108–16.
34. Jacobs MA, Ouwerkerk R, Wolff AC, Gabrielson E, Warzecha H, Jeter S, et al. Monitoring of neoadjuvant chemotherapy using multiparametric, (23)Na sodium MR, and multimodality (PET/CT/MRI) imaging in locally advance breast cancer. Breast Cancer Res Treat. 2011;128:119–26.
35. Loo CE, Straver ME, Rodenhuis S, Muller SH, Wesseling J, Vrancken Peeters MJ, et al. Magnetic resonance imaging response monitoring of breast cancer during neoadjuvant chemotherapy: relevance of breast cancer subtype. J Clin Oncol. 2011;29:660–666.
36. Wang B, Povoski SP, Cao X, Sun D, Xu RX. Dynamic schema for near infrared detection of pressure-induced changes in solid tumors. Appl Opt. 2008;47:3053–63.